Microelectronics Reliability 52 (2012) 2744–2748

Contents lists available at SciVerse ScienceDirect

Microelectronics Reliability

journal homepage: www.elsevier.com/locate/microrel

Effect of EFO parameters and superimposed ultrasound on work hardening behavior of palladium coated copper wire in thermosonic ball bonding

W.H. Song [a,*], M. Mayer [a], Y. Zhou [a], S.H. Kim [b], J.S. Hwang [b], J.T. Moon [b]

[a] Microjoining Laboratory, Centre for Advanced Materials Joining, Department of Mechanical and Mechatronics Engineering, University of Waterloo, Waterloo, Ontario, Canada N2L 3G1

[b] MK Electron Co. Ltd., 316-2 Geumeo-ri Pogok-eup Cheoin-gu Yongin-si, Gyeonggi-do 449-812, Republic of Korea

ARTICLE INFO

Article history:
Received 5 December 2011
Received in revised form 26 March 2012
Accepted 27 March 2012
Available online 1 May 2012

ABSTRACT

Effects of the electrical flame off (EFO) and ultrasound (US) parameters on the work hardening behavior of Pd coated Cu (PCC) free air ball (FAB) are presented and compared to those of bare Cu reported in the literature. The FABs are characterized using an online deformability method that measures in situ deformed ball height (H_{DEF}). The levels of EFO current (I_{EFO}) of 65, 100 and 160 mA with adjusted EFO time (t_{EFO}) are used to make 40 μm diameter FABs in two different shielding gases, resulting in six experimental conditions. In a first experiment, a total of 135 samples are produced for each condition and then deformed under a 400 mN deformation force (F_D) without superimposing US. PCC FABs produced in nitrogen gas using I_{EFO} and t_{EFO} of 160 mA and 0.120 ms, respectively, are more deformable, having H_{DEF} 7.1–9.2% less compared to those produced with I_{EFO} = 100 mA and t_{EFO} = 0.218 ms. However, the FABs produced with the higher current vary more than those with lower current, and FABs produced with forming gas vary least. H_{DEF} of PCC FABs made in forming gas is independent of I_{EFO} in the range from 65 to 160 mA. In a second experiment, the same conditions are used except for a 20% US level (equivalent to 29 mW US power) superimposed on F_D during the deformation. The values of H_{DEF} with US is 5.7–11.7% and 6.5–9.0% smaller than those of without US for the I_{EFO} ranging from 65 to 160 mA in nitrogen and forming gas, respectively.

1. Introduction

The thermosonic wire bonding has been most widely used as a first level interconnection technology for IC packaging [1]. Traditionally, Au is predominantly used as bonding wire due to its proven reliability and corrosion resistance. However, the soaring price of Au is pushing the packaging industry to use Cu as an alternative material [1–3]. However, in comparison to Au, Cu as a bonding wire has limitations such as (a) a reduced second bond process window and (b) its higher hardness which can cause underpad damages. To overcome the first of these limitations, Pd has been introduced as a coating that expands the second bond process window [4–7]. PCC wire works fine with the conventional forming gas ($N_2 + 5\%H_2$) used for bare Cu wire, and also is used with nitrogen gas which is more cost effective but does not work with bare Cu wire. Cost comparison of wire's materials are summarized in Table 1. Although the cost of raw Pd is 42% of Au, the cost of PCC wire per 1 km is 0.53% of Au wire because the Pd thickness is only 100 nm.

As Cu and PCC FABs are harder than Au FABs, larger underpad stresses occur during ball bonding, increasing the risk of underpad damage. Several different approaches have been explored to reduce underpad stress: Softer wire, producing softer FABs, optimizing the bonding parameters, and modifying the bond pad design are used to limit underpad damage [1,8,9]. Cu bonded ball [9] and Cu FABs [10] with different hardness can be obtained by changing EFO parameters and temperature of the shielding gas. The increase of EFO current shows decrease of FAB work hardening during the deformation in Cu wire [11,12]. Also, US can induce a decrease of FAB working hardening of Cu wire [13,14].

In the current study the effects of EFO and US parameters on the deformability of FAB of PCC wire are examined. The better understanding gained from the new results can lead to easier adaptations of PCC wire in large scale productions.

2. Experimental

A 99.99% purity 20 μm diameter Cu wire coated with approximately 100 nm of Pd manufactured by MK Electron Co. Ltd., Yongin, Korea, is used on an automatic wire bonder 3100 (Esec Ltd., Cham, Switzerland) with an ultrasonic vibration frequency of 128 kHz for bonding and characterization of the FAB properties. A capillary with hole diameter of 28 μm, face angle of 11°, chamfer angle of 90°, and chamfer diameter of 35 μm is used. A number of Ag plated diepads of standard PLCC44 leadframes are used as bonding substrates.

* Corresponding author. Tel.: +1 519 888 4567 x38579; fax: +1 519 885 5862.
E-mail address: wanho@uwaterloo.ca (W.H. Song).

0026-2714/$ - see front matter
http://dx.doi.org/10.1016/j.microrel.2012.03.030

Table 1
Cost comparison of bonding wires based on raw metal market price [18].

Raw material	Cu	Pd	Au	Ag
Cost/kg (USD)	8.60	24.569	58.339	1.133
20 μm bonding wire	Cu	PCC (100 nm Pd coating)	Au	Ag
Raw material cost/km (USD)	0.024	1.87	353.72	3.73

Table 2
Main nominal EFO time parameter for measurement of FAB deformability (ms).

	I_{EFO} (mA)		
	65	100	160
Shielding gas			
N_2	0.380	0.218	0.120
$N_2 + 5\%H_2$	0.340	0.208	0.130

The I_{EFO} and t_{EFO} levels used in this study are summarized in Table 2. The bonding parameters are summarized in Table 3.

A fixed deformation force of F_D = 400 mN is used for the controlled deformation of the FABs. The previously reported on-line method is used to evaluate FAB deformability by measuring FAB height (H_{FAB}) as illustrated in Fig. 1a and b, and deformed FAB height (H_{DEF}) [11–16].

2.1. FAB deformability without superimposed US

The evaluation procedure for FAB deformability without superimposed US is carried out in two steps:

1. Deform FAB samples with controlled deformation force to determine deformed ball heights for various I_{EFO} levels. H_{FAB} is also recorded for each sample.
2. From the results of the previous step, a correction factor is determined and used to find H_{DEF} values that are corrected for H_{FAB} variations.

In step 1, three sets of 45 FAB samples are produced (135 samples in total) for each of the six conditions (18 sets in total). The values of H_{FAB} and H_{DEF} are obtained. In step 2, the correction factor is extracted from the relationship between mean values (without outliers) of deformed ball height versus a range of H_{FAB} and applied to find H_{DEF} (corrected) as described in [16].

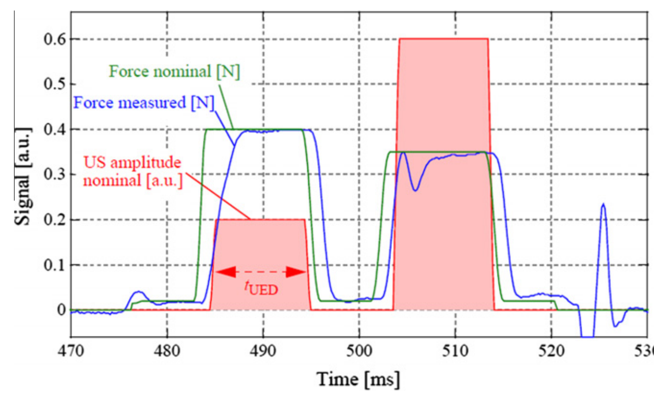

Fig. 2. Example parameter profiles recorded by wirebonder-PC during test ball bond.

2.2. FAB deformability with superimposed US

The influence of US on the FAB deformability is investigated in a similar way as described in [13,14]. The evaluation procedure described in the previous subsection is modified to include ultrasound during FAB deformation. A US level of 20% is now used during the FAB deformation as shown graphically in the profiles of Fig. 2. H_{DEF}

Table 3
Main nominal bonding parameters.

	Parameters								
	Shielding gas		Ball bonding			Wedge bonding			Stage
	Type	Flow rate (l/min)	Force (mN)	Ultrasound (%)	Time (ms)	Force (mN)	Ultrasound (%)	Time (ms)	Temperature (°C)
Values	N_2 or $N_2 + 5\%H_2$	0.5	350	50	9.9	350	30	9.9	220

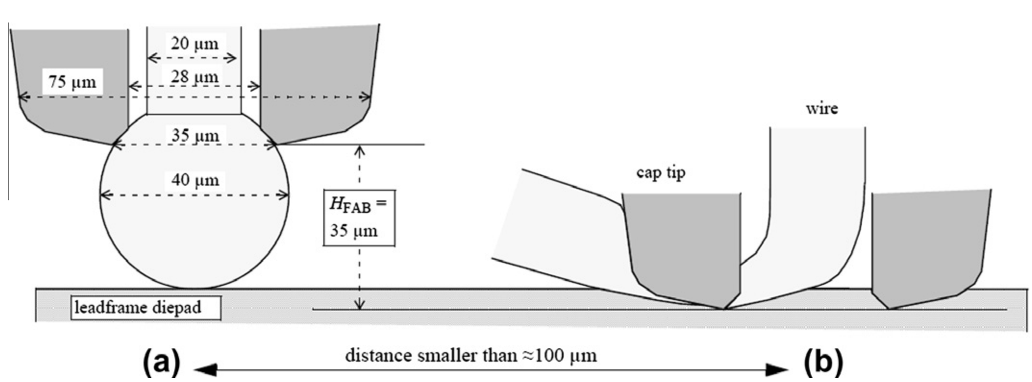

Fig. 1. Measurement principle for H_{FAB} with online method using z-position signal of wirebonder: (a) after soft-touchdown and (b) after second bond to measure reference position. Note that capillary tip is expected to sink into substrate during second bond, leaving an imprint.

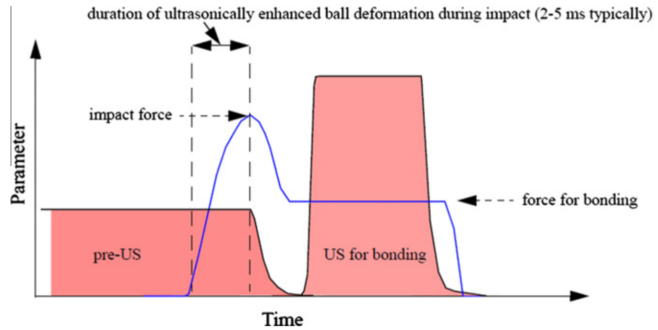

Fig. 3. Schematic of typical parameter profiles during industrial ball bond with pre-US.

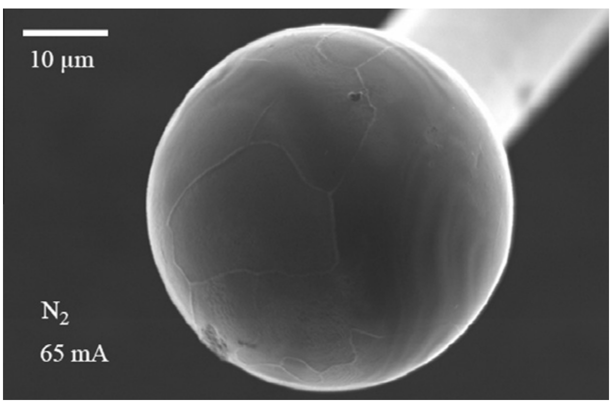

Fig. 4. SEM image of PCC FAB with diameter ≈40 μm made with 65 mA and 0.38 ms of EFO current and time, respectively, under N_2 shielding.

due to a smaller or larger US level than 20% will be shadowed by or shadowing the effect of I_{EFO} on H_{DEF}, respectively.

Compared to a typical bonding process, these profiles exaggerate the influence of ultrasound as the duration of ultrasonically enhanced deformation (t_{UED}) is 9.9 ms, i.e. substantially larger than in a typical process with pre-ultrasound (pre-US, pre-bleed) where the t_{UED} is approximately 2–5 ms, and profiles can look like those shown in Fig. 3.

3. Results and discussion

Each of the six conditions produces 40 μm diameter FABs in average and Fig. 4 shows a typical FAB made using I_{EFO} = 65 mA and t_{EFO} = 0.38 ms under N_2 shielding. The significance of differences resulted using different conditions such as EFO and US superimposition are calculated using 95% confidence interval t-test.

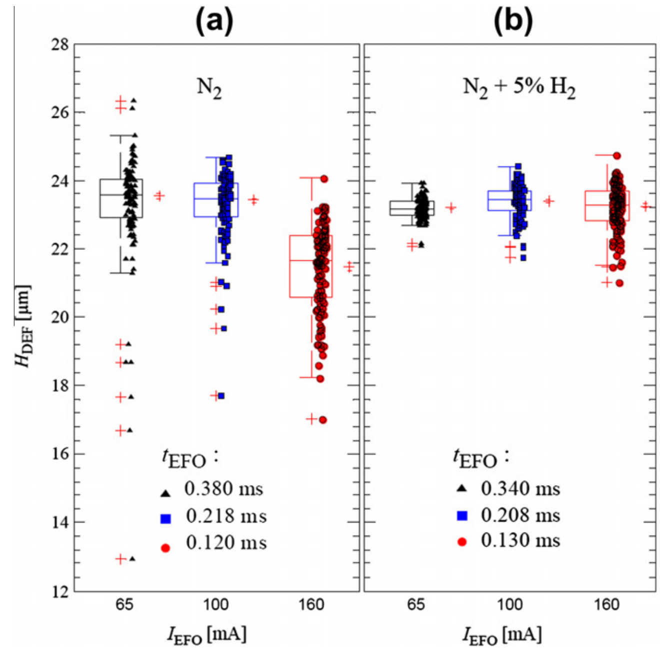

Fig. 5. Corrected ball height deformed with 400 mN for different EFO current levels. Mean and standard error values (obtained without outliers) are on right next to each box plot. Shielding gas: (a) N_2 and (b) forming gas.

3.1. Deformed ball height without superimposed US

Measured values for H_{DEF}, are given in Table 4 and shown in Fig. 5a and b for N_2 and forming gas, respectively. The outliers (6% of measurements in case of I_{EFO} = 65 mA and with N_2 shielding) in Fig. 5a and b are due to mis-shaped (golf clubbed or pointed) FABs. The deformability of FABs made in forming gas is independent of I_{EFO}, possibly due to the formation of a hard phase such as palladium hydride [17].

The H_{DEF} of FABs made in N_2 with I_{EFO} = 160 mA is 7.1–9.2% smaller (ΔH_{DEF} = 1.95 μm) than that of made with 100 mA. Thus, the FAB deformability is increased when I_{EFO} is increased. This result is similar to the results obtained previously [11,12] where deformability of constant diameter Cu FABs increased with the increase of I_{EFO}. In [16], the correlation between force-to-target-deformation and H_{DEF} is studied. Similarly here, the increase in deformability is expressed by the drop of deformation force require to obtain the same amount of deformation,

$$\Delta F_D = s \times \Delta H_{DEF} = 97.87 \text{ mN}, \qquad (1)$$

where s = 50.2 mN/μm is the calibration factor [16].

The standard error of the H_{DEF} is also increased with increase of I_{EFO}, similar to the results obtained previously [12].

3.2. Deformed ball height with superimposed US

Measured values for H_{DEF}, are given in Table 5 and shown in Fig. 6a and b for N_2 and forming gas, respectively.

Table 4
Corrected ball height deformed with 400 mN (average ± standard error after removing outliers).

Shielding gas	PCC wire N_2			$N_2 + 5\%H_2$		
EFO current (mA)	65	100	160	65	100	160
Correction factor (K)	1			0.95		
Corrected deformed ball height (μm)	23.53 ± 0.07	23.41 ± 0.06	21.46 ± 0.11	23.19 ± 0.03	23.40 ± 0.04	23.24 ± 0.06

Table 5
Corrected ball height deformed with 400 mN and 20% US (average ± standard error after removing outliers).

Shielding gas	PCC wire					
	N_2			$N_2 + 5\%H_2$		
EFO current (mA)	65	100	160	65	100	160
Correction factor (K)	1			1.2		
Corrected deformed ball height (μm)	22.02 ± 0.04	21.42 ± 0.05	19.34 ± 0.16	21.60 ± 0.03	21.45 ± 0.07	21.57 ± 0.07

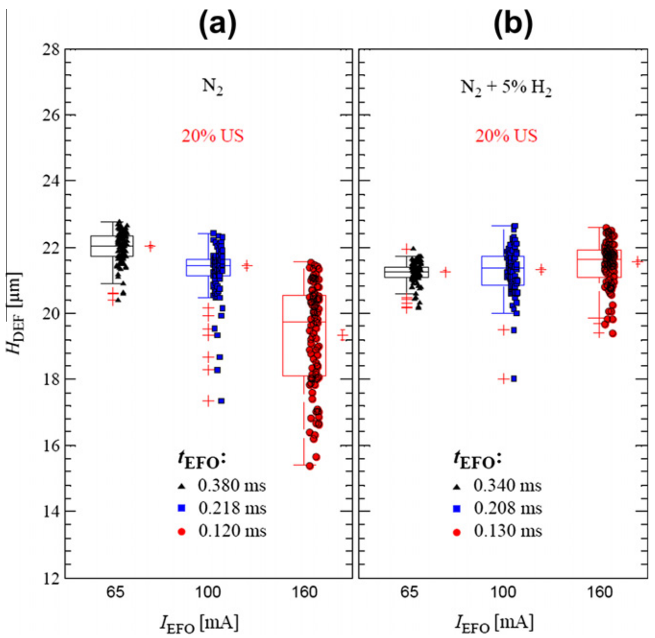

Fig. 6. Corrected ball height deformed with 400 mN and 20% US for different EFO current levels. Mean and standard error values (obtained without outliers) are on right next to each box plot. Shielding gas: (a) N_2 and (b) forming gas.

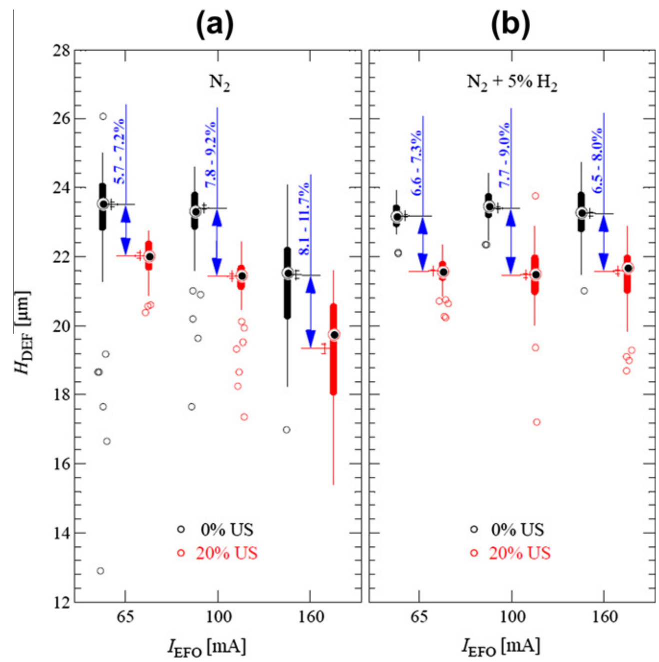

Fig. 7. Comparison of deformed ball height (corrected) for different EFO current with superimposed 20% US (red data) and without US (black data). Change statistics are indicated in percentage with blue color (95% confidence interval, outliers excluded). Shielding gas: (a) N_2 and (b) forming gas. (For interpretation of the references to color in this figure legend, the reader is referred to the web version of this article.)

The results are lower than those without superimposed US but show similar trends. No work hardening effect observed with 20% of US level superimposed during the deformation.

3.3. Comparison between with and without superimposed US

H_{DEF} is significantly reduced due to superimposed US. The statistical significance is computed using t-test. Data is summarized in Table 6 and shown in Fig. 7a and b.

With N_2 during EFO and 20% US during deformation, the average H_{DEF} is 5.7–11.7% smaller than without US for I_{EFO} ranging from 65 to 160 mA. With forming gas and superimposed US, the average H_{DEF} is 6.5–9.0% smaller than without US for the same I_{EFO} range. The overlapping ranges of H_{DEF} reduction indicate that there is no significant interaction between the effects of I_{EFO} and superimposed US on FAB deformability.

The H_{DEF} value of the FABs deformed with 20% US is 1.75 and 1.87 μm smaller in ΔH_{DEF} on average for N_2 and forming gas, respectively, than that of the FABs deformed without US. With $\Delta F_D = s \times \Delta H_{DEF}$ and s = 50.2 and 57.9 mN/μm for N_2 and forming gas, respectively [16], the force needed to reach the same deformed height is approximately 25% less than without US.

4. Conclusions

The effects of EFO current and superimposed US on deformation of FAB made of PCC wire are substantial. There is a trade-off between more deformable FABs and FABs with lower variation. While FABs formed in N_2 with high current seem most deformable, their variation is highest which still may lead to underpad damage. To control underpad stress in thermosonic bonding of PCC wire, high deformability and small FAB variation need to be considered at the

Table 6
Comparison of deformed ball height (corrected) between superimposed ultrasound and no ultrasound (average ± standard after removing outliers).

Shielding gas	PCC wire					
	N_2			$N_2 + 5\%H_2$		
EFO current (mA)	65	100	160	65	100	160
no-US (μm)	23.53 ± 0.07	23.41 ± 0.06	21.46 ± 0.11	23.19 ± 0.03	23.40 ± 0.04	23.24 ± 0.06
20% US (μm)	22.02 ± 0.04	21.42 ± 0.05	19.34 ± 0.16	21.60 ± 0.03	21.45 ± 0.07	21.57 ± 0.07
Reduction (%)	5.7–7.2	7.8–9.2	8.1–11.7	6.6–7.3	7.7–9.0	6.5–8.0

same time. In all cases, the superposition of ultrasound during the deformation results in less force required for the same amount of deformation, potentially leading to less underpad stress during bonding.

Acknowledgments

This work is supported by the MK Electron Co. Ltd., Yongin, Korea, the Natural Science and Engineering Research Council (NSERC) Canada, and Initiative for Automotive Manufacturing Innovation (IAMI), Ontario, Canada.

References

[1] Harman GG. Wire bonding in microelectronics. 3rd ed. New York: McGraw Hill; 2010.
[2] Khoury S, Burkhard DJ, Galloway DP, Scharr TA. A comparison of copper and gold wire bonding on integrated circuit devices. IEEE Trans Compon Hybr Manufact Technol 1990;13(4):673–81.
[3] Ellis TW, Levine L, Wicen R. Copper: emerging material for wire bond assembly. Solid State Technol 2000;43(4):71–7.
[4] Uno T, Terashima S, Yamada T. Surface-enhanced copper bonding wire for LSI. In: Proc 59th electronics components and technology conference; 2009. p. 1486–95.
[5] Zhang B, Qian K, Wang T, Cong Y, Zhao M, Fan X, et al. Behaviors of palladium coated copper wire bonding process. In: Proc inter conference electronic packaging technology and high density packaging; 2009. p. 662–5.
[6] Uno T. Enhancing bondability with coated copper bonding wire. Microelectron Reliab 2011;51:88–96.
[7] Uno T. Bond reliability under humid environment for coated copper wire and bare copper wire. Microelectron Reliab 2011;51:148–56.
[8] Shah A, Mayer M, Zhou Y, Hong SJ, Moon JT. Reduction of underpad stress in thermosonic copper ball bonding. In: Proc. of the 58th electronics components and technology conference; 2008. p. 2123–30.
[9] Zhong ZW, Ho HM, Tan YC, Tan WC, Goh HM, Toh BH, et al. Study of factors affecting the hardness of ball bonds in copper wire bonding. Microelectron Eng 2007;84:368–74.
[10] Onuki J, Koizumi M, Suzuki H. Influence of ball forming conditions on the hardness of copper balls. J Appl Phys 1990;68:5610–4.
[11] Hang CJ, Song WH, Lum I, Mayer M, Zhou Y, Wang CQ, et al. Effect of electronic flame off parameters on copper bonding wire: free-air ball deformability, heat affected zone length, heat affected zone breaking force. Microelectron Eng 2009;86:2094–103.
[12] Pequegnat A, Hang CJ, Mayer M, Zhou Y, Moon JT, Persic J. Effect of EFO parameters on Cu FAB hardness and work hardening in thermosonic wire bonding. J Mater Sci: Mater Electron 2009;20:1144–9.
[13] Huang H, Pequegnat A, Chang BH, Mayer M, Du D, Zhou Y. Influence of superimposed ultrasound on deformability of Cu. J Appl Phys 2009;106:113514.
[14] Lum I, Hang CJ, Mayer M, Zhou Y. In situ studies of the effect of ultrasound during deformation on residual hardness of a metal. J Electron Mater 2009;38:647–54.
[15] Hang CJ, Lum I, Lee J, Mayer M, Wang CQ, Zhou Y, et al. Bonding wire characterization using automatic deformability measurement. Microelectron Eng 2008;85:1795–803.
[16] Rezvani A, Mayer M, Shah A, Zhou N, Hong SJ, Moon JT. Free-air ball formation and deformability with Pd coated Cu wire. In: Proc. of the 61st electronics components and technology conference; 2011. p. 2123–30.
[17] Grochala W, Edwards PP. Thermal decomposition of the non-interstitial hydrides for the storage and production of hydrogen. Chem Rev 2004;104:1283–315.
[18] http://www.infomine.com/investment/metal-prices/.